

25th International Conference on Prenatal Diagnosis and Therapy

23-26 May 2021 • Edinburgh, UK



Save the dates and join ISPD next year, either in person or through virtual conferencing, for another great conference!

Preconference courses, invited talks, abstract presentations and posters will cover the cutting edge of clinical genetics, fetal imaging, and fetal therapy.

www.ispdhome.org/2021



ispd International Society
for Prenatal Diagnosis

Building Global Partnerships in Genetics and Fetal Care

A global society with a membership of more than 400 professionals from multiple disciplines such as prenatal and perinatal care, medical genetics, basic and translational science, genetic counseling, laboratory management, fetal therapy, ultrasonography, and ethics

Membership is complimentary for students and trainees.



www.ispdhome.org
info@ispdhome.org
+1 434.979.4773

Potential sealing and repair of human FM defects after trauma with peptide amphiphiles and Cx43 antisense

David W. Barrett¹ | Babatunde O. Okesola¹ | Eleni Costa¹ |
Christopher Thrasivoulou² | David L. Becker³ | Alvaro Mata^{1,4} |
Jan A. Deprest^{5,6}  | Anna L. David^{5,6,7} | Tina T. Chowdhury¹ 

¹Institute of Bioengineering, School of Engineering and Materials Science, Queen Mary University of London, London, UK

²Department of Cell and Developmental Biology, University College London, London, UK

³Lee Kong Chian School of Medicine, Nanyang Technological University, Singapore, Singapore

⁴Biodiscovery Institute, School of Pharmacy, Department of Chemical and Environmental Engineering, University of Nottingham, Nottingham, UK

⁵Department of Obstetrics and Gynecology, University Hospitals Leuven, Leuven, Belgium

⁶Institute for Women's Health, University College London, London, UK

⁷NIHR University College London Hospitals Biomedical Research Centre, London, UK

Correspondence

Tina T. Chowdhury, Institute of Bioengineering, School of Engineering and Materials Science, Queen Mary University of London, Mile End Road, London E1 4NS, UK.
Email: t.t.chowdhury@qmul.ac.uk

Funding information

Great Ormond Street Hospital for Children, Grant/Award Number: 17QMU01; Rosetrees Trust, Grant/Award Number: M808

Abstract

Objective: We examined whether peptide amphiphiles functionalised with adhesive, migratory or regenerative sequences could be combined with amniotic fluid (AF) to form plugs that repair fetal membrane (FM) defects after trauma and co-culture with connexin 43 (Cx43) antisense.

Methods: We assessed interactions between peptide amphiphiles and AF and examined the plugs in FM defects after trauma and co-culture with the Cx43antisense.

Results: Confocal microscopy confirmed directed self-assembly of peptide amphiphiles with AF to form a plug within minutes, with good mechanical properties. SEM of the plug revealed a multi-layered, nanofibrous network that sealed the FM defect after trauma. Co-culture of the FM defect with Cx43 antisense and plug increased collagen levels but reduced GAG. Culture of the FM defect with peptide amphiphiles incorporating regenerative sequences for 5 days, increased F-actin and nuclear cell contraction, migration and polarization of collagen fibers across the FM defect when compared to control specimens with minimal repair.

Conclusions: Whilst the nanoarchitecture revealed promising conditions to seal iatrogenic FM defects, the peptide amphiphiles need to be designed to maximize repair mechanisms and promote structural compliance with high mechanical tolerance that maintains tissue remodeling with Cx43 antisense for future treatment.

1 | INTRODUCTION

Strategies to seal and repair defects in the fetal membrane (FM) after fetal surgery are important to prevent iatrogenic preterm prelabour rupture of the membranes (PPROM). After open fetal surgery, membranes separate in up to 30% of patients commonly leading to PPRM and preterm birth.¹ Even after fetoscopy which results in trauma, the membranes do not heal and a visible defect is left in the FM that is

prone to AF leakage and subsequent iatrogenic PPRM.¹ The subsequent preterm birth compromises the outcome of treatment, reducing the clinical effectiveness of fetal surgery.² Currently, there are no clinical solutions to improve healing of the FM after trauma or rupture.

Several novel sealing techniques are aiming to restore a physical barrier against infection encouraging re-accumulation of AF. The approaches either (a) seal the FM defect with natural, synthetic or injectable materials such as plugs, films, sponge, patches, sealants and

This is an open access article under the terms of the Creative Commons Attribution License, which permits use, distribution and reproduction in any medium, provided the original work is properly cited.

© 2020 The Authors. *Prenatal Diagnosis* published by John Wiley & Sons Ltd.

glues or (b) heal the FM defect with therapeutics to induce repair mechanisms. For example, platelet or fibrin-based strategies, gelatin or collagen plugs, cyanoacrylate or surgical glues are limited however, with around 51% to 61% fetal survival rate.³⁻⁷ Strategies with collagen with fibrinogen plugs in the mid-gestational rabbit model, or from porcine small intestine and decellularised human amnion are imperfect.⁸⁻¹⁰ Many of these approaches suffer from poor adhesion to wet tissues, mismatch of mechanical properties, rapid swelling or degradation due to protease activity in the AF, cytotoxicity, and severe iatrogenic complications. Whilst mussel-mimetic tissue adhesives strongly adhere to elastomeric membranes and demonstrate good adhesion under wet conditions without swelling, degradation, cytotoxicity, it is not known whether the repaired FM defect could support mechanical loads and withstand the repetitive effects of mechanical stretch or inflation applied by a bioreactor device long term.¹¹⁻¹⁴ Interestingly, the ex-vivo tested mussel glue sealed fetal membranes and resisted pressures achieved during uterine contractions show promising results.¹² Future developments for sealants or plugs require strong adherence capabilities that maintain mechanical resilience and tissue function long-term.

We and others have shown that targeting connexin 43 (Cx43) with antisense in stretched, wounded or inflamed tissues improves cell proliferation and migration rates leading to healing mechanisms and wound closure.¹⁵⁻¹⁸ Growth and healing mechanisms can be promoted with AF derived stem cells supplemented with AF alone or in combination with alginate, silk or fibroin fibers to heal a variety of tissues.¹⁹⁻²² Peptide amphiphiles (PAs) conjugated with ligands for cell-adhesion (RGDS), migratory (GHK), or regenerative (GHK/RGDS) peptides can be assembled with synovial fluid, blood serum, albumin, salts or DNA to generate nanostructured fibers with spatio-temporal control and tunable functionalities.²³⁻²⁵ Here we examined in vitro whether combining AF with PA solutions modified to incorporate sequences that enhance adhesion, cell migration or regeneration could repair FM defects after trauma.

2 | METHODS

All methods were performed according to the relevant guidelines and regulations at University College London Hospital and the School of Engineering and Materials Science, Queen Mary University of London. Ethical approval for amniotic fluid and fetal membrane sample collection was granted by the Joint UCL and UCLH Committees and the Ethics of Human Research Central Office (REC reference: 14/LO/0863). All patients gave written consent to provide AF and FM tissue samples before procedures were performed.

2.1 | Amniotic fluid collection

The human AF samples were collected from women undergoing fetoscopic laser ablation of placental vascular anastomoses for treatment of twin-to-twin transfusion syndrome (TTTS) in mid-trimester pregnancies ($n = 6$) or fetal surgery for open spina bifida ($n = 2$) or amniocentesis for fetal diagnostic genetic testing ($n = 1$). All fetuses

What is already known about this topic?

- After fetal surgery, the human fetal membrane shows limited healing and overexpression of Cx43 at the wound edge.
- The evidence for the sealing and repair of iatrogenic membrane defects and restoration of fetal membrane function with biomaterials is variable with conflicting data on their ability to prevent amniotic fluid leakage, infection and rupture.

What does this study add?

- We explored the in vitro molecular assembly of peptide amphiphiles with human amniotic fluid to potentially seal and repair defects in the fetal membrane after trauma and co-culture with the Cx43 antisense.
- We showed that functionalizing the peptide amphiphiles with bioactive sequences to promote cell adhesion, migration and regeneration or culturing with Cx43 antisense improves sealing and the repair of defects in the fetal membrane.

had a normal karyotype. AF ranged from 16 + 1 to 24 + 0 weeks of gestation with a maternal age from 27 to 33 years. All AF samples were immediately stored at -20°C until the experiments could be performed. Each experiment was repeated at least three times with AF samples collected from a minimum of three separate donors.

2.2 | Fetal membrane collection

Women gave informed consent for term human placentas ($n = 12$) to be collected after elective cesarean delivery at University College London Hospital. Women with placenta praevia, multiple pregnancy, antepartum hemorrhage, PPRM or small for gestational age were excluded from the study. The placenta was carefully separated from the uterus and the FM was rinsed with Earle's Balanced Salt Solution (EBSS), as described.²⁶ FM were dissected into 25×25 mm explants, washed with EBSS and equilibrated in DMEM +20% FCS for 24 hours.

2.3 | Synthesis and characterization of peptides

The PAs (PAK2, PAK3, PAK4 and PAH3) were synthesized using solid phase peptide synthesis (SPPS) on a Liberty Blue automated microwave peptide synthesizer (CEM, UK) and characterized by electrospray ionization mass spectrometry (ESI-MS), as described.^{27,28} The PAK3 molecules were modified to incorporate the cell-adhesion peptide arginine-glycine-glutamic acid-serine (RGDS), migratory (GHK) or regenerative (GHK/RGDS) peptides. Purification of the PAs were carried out using a 2545 binary gradient HPLC with a 2489 UV/Visible detector on the C18 column (Atlantis Prep OBD T3 Column, Waters, USA) and a water/acetonitrile (0.1% TFA) gradient. The

PA solutions were lyophilized and stored at -20°C (Yield = 85% and Purity = 95% by HPLC).

2.4 | Early stage PAK3 development using a PDMS device

A well-established polydimethylsiloxane (PDMS) capillary device was used to investigate the interactions of the PAK3 solution and the AF sample during early plug development, as described.²⁹ Human AF sample (90 μL) was injected into one end of the PDMS device and the PAK3 solution (10 μL , 2%) was added to the opposite end. The structural plug formation and interactions at the interface of the PAK3 solution and the AF specimen were examined by light and confocal microscopy and imaging with time-lapse of the fluorescently labeled PAK3-TAMRA on an epifluorescence microscope (Leica, DMI 4000B).

2.5 | Treatment of FM defects after trauma

We used an established in vitro FM defect model (Figure 1) to examine the effects of PAK application after trauma.¹⁷ A 21 Gauge needle was used to create a 0.8 mm diameter defect in the FM secured within the crown insert of a 24 well plate (Figure 1A-C). Human AF (1 mL) was injected into the well below the FM explant (Figure 1D). Solutions of the PAK3, PAK3/GHK, PAK3/RGDS or PAK3/GHK/

RGDS (2%) prepared in HEPES buffer (10 mM) with 0.01 M NaCl (pH 7.4) were applied to the surface of the FM defect and cultured for up to 5 days with AF replaced every 48 hours (Figure 1E). In separate experiments, FM defects were cultured with PAK3 alone or in the presence and absence of 0 or 50 μM Cx43 antisense (Cx43as) for 48 hours. At the end of the experiment, the FM specimens were either fixed in 4% PFA or stored at -20°C prior to analysis.

2.6 | Electron microscopy

We evaluated the macrostructure of the PAK3 plugs by Scanning Electron Microscopy (SEM) after early (30 seconds, 2 minutes) and late fixation (24 hour). After each time point, the PAK3 plugs were fixed in 4% PFA, washed with Milli-Q water before being passed through a graded ethanol series (20-100% v/v) and dried to critical point (K850, Quorum Technologies, UK). Specimens were mounted on 10 mm SEM mounting blocks and sputter coated with 10 nm gold particles prior to SEM using an FEI Inspect-F50 (FEI Comp, The Netherlands).

2.7 | Mechanical testing

The mechanical behavior of the PA solutions after assembly with the AF specimens were measured in situ by dynamic oscillatory rheology using a Discovery Hybrid Rheometer (Rheo-DHR3, TA Instruments, USA), as

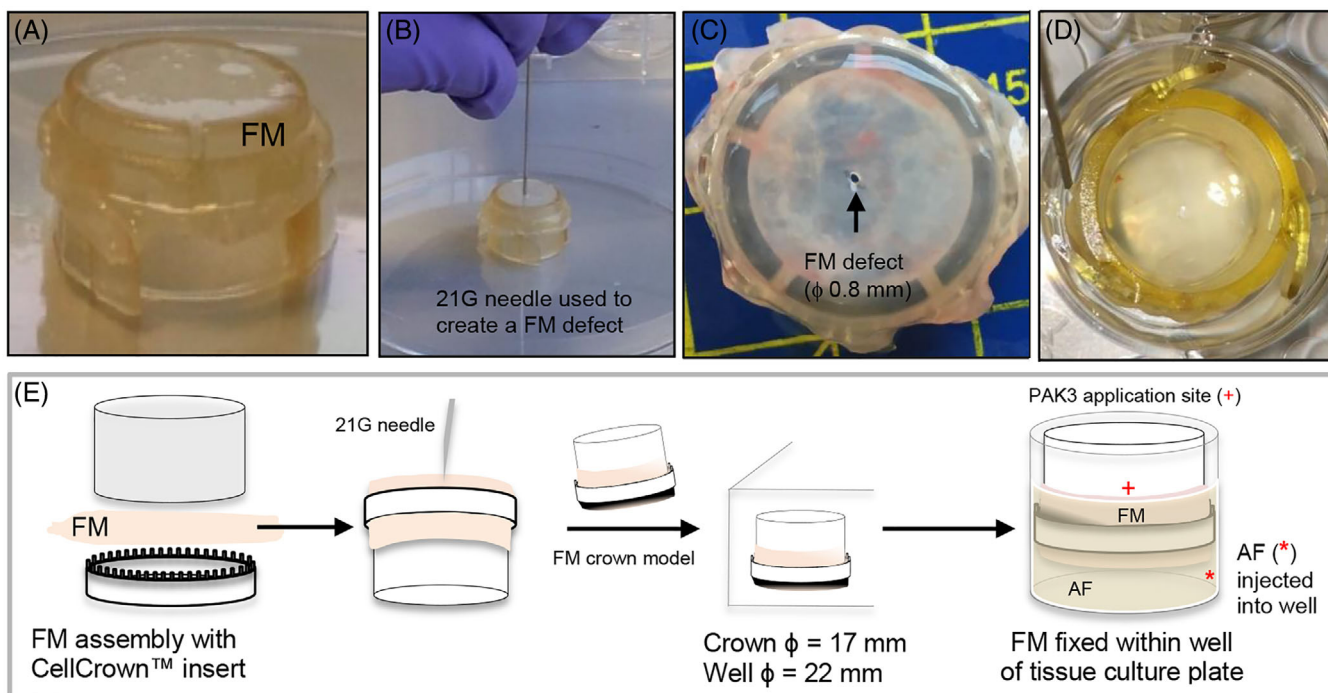


FIGURE 1 In vitro fetal membrane defect model. Fetal membranes (FM) were collected from term placentas from women undergoing elective cesarean section between 37 and 42 weeks of gestation. The FM was excised into tissue explants (25 \times 25 mm) and assembled with the CellCrown insert (A). A 21 Gauge needle was used to create a 0.8 mm diameter defect in the FM explant (B and C). The FM crown model was transferred into the well of a tissue culture plate and amniotic fluid (AF) injected into the well (D), to cover the area below the FM explant. The * indicates AF injection site and + indicates PAK3 application site (E) [Colour figure can be viewed at wileyonlinelibrary.com]

previously described.³⁰⁻³² The Storage (G') and Loss Modulus (G'') of the resultant plug were assessed for specimens at oscillatory strain rates (0.1%-100%) and varying time periods (100, 200-400 seconds). In a separate set of experiments, time sweep measurements were conducted at constant frequency (1 Hz) whilst strain sweeps were performed from 0.1% to 1000% strain for 3 hours to determine the strain to break value.

2.8 | Biochemical assays

Total glycosaminoglycan (GAG), DNA and collagen content were measured in papain or pepsin digested samples using the well-established DMMB, Hoechst and hydroxyproline assays.^{18,26}

2.9 | Cell viability

After PA treatment, FM explants were incubated with calcein AM and ethidium homodimer (both 5 μ M, Invitrogen, Paisley, UK) for

45 minutes at 37°C and were visualized by fluorescence microscopy using an $\times 20$ objective (Leica, Milton Keynes, UK). Live and dead cells were imaged from different fields of view of ~ 0.5 mm² to calculate the percentage cell viability.

2.10 | Histological analysis

FM explants were fixed in 4% PFA and embedded in paraffin. Sections (5 μ m) were stained with hematoxylin and eosin (H&E), as described.¹⁷

2.11 | IMF confocal microscopy and SHG imaging

Specimens were imaged using two photon confocal imaging on a Leica SP8 with a Coherent Chameleon Ultra, Ti Sapphire mode locked IR laser (Leica, Milton Keynes, UK), as described.¹⁷ Tissues were stained with the nuclear dye DAPI (1:1000, Roche) and F-actin Flash

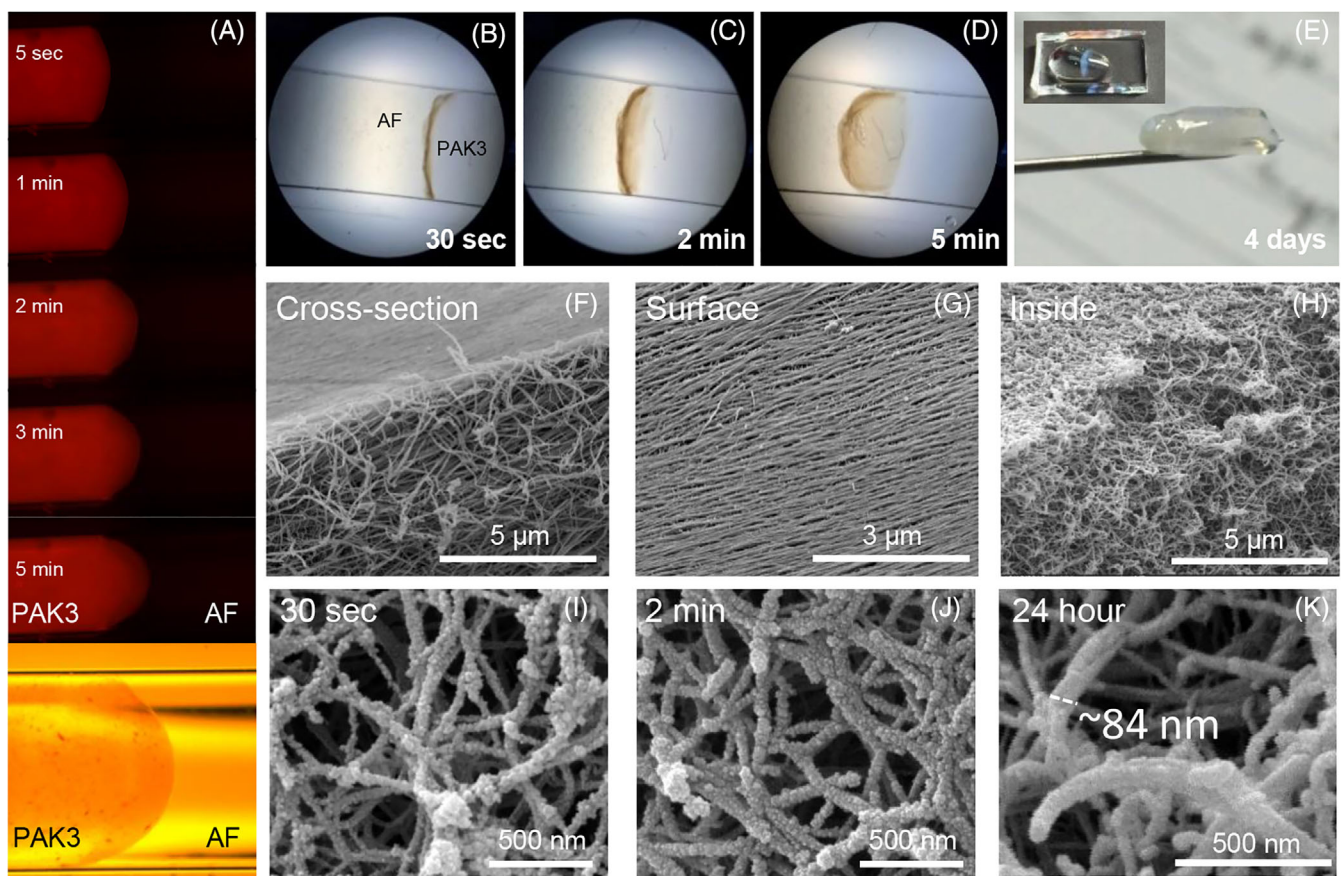


FIGURE 2 Temporal and structural properties of the PAK3 and AF plug. A well-established PDMS channel model was used to investigate the interaction of the PAK3 solution with the AF sample. Confocal and light microscopy (A), confirmed directed self-assembly of PAK3 solution with the AF sample to form an interfacial membrane region within 30 seconds (B), 2 minutes (C), 5 minutes (D), and formed a plug that remained stable up to 4 days in the AF sample (E). Cross-sectional analysis of the PAK3 plug revealed a multi-layered hierarchical structure F, with highly aligned nanofibres on the surface G, and a randomly arranged network inside the plug H. Higher magnification confirmed an interconnected network of the individual and bundled nanofibres after early J and K, and late fixation K. Scale bars are indicated by the white lines. All interactions were repeated at least six times with mid-trimester AF taken from six donors. The AF sample presented in the images was taken from one donor at 19 + 3 weeks of gestation [Colour figure can be viewed at wileyonlinelibrary.com]

Phalloidin (1:1000, Merck) and the samples were imaged at excitation/emission wavelengths of 405/460 nm and 495/518 nm, respectively. A transmission detector was used to collect the SHG signal for collagen with a 430 to 450 nm barrier filter with a pump wavelength of 880 nm at 80 fs pulse width. A constant step size (Z-section interval) of 1.5 μm was used across all Z-stack images collected. All parameters including detector gain, offset and laser power were kept constant. Images were processed using ImageJ software (64bit), as described.¹⁷

2.12 | Statistical analysis

All values are expressed as the mean and \pm SEM. Statistical comparisons for the multiple groups were performed using a post hoc Bonferroni-corrected *t*-test where values of $P < .05$ were considered statistically significant. The number of replicates for each test condition from separate donors are indicated in the figure legend.

3 | RESULTS

3.1 | Early stage co-assembly of PAK3 with AF

Structural evolution at the interface of the PAK3 solution and AF sample were investigated using a well-established PDMS channel model (Figure 2). Time-lapse imaging with confocal and light microscopy confirmed rapid directed self-assembly of PAK3 to form a structural interface which occurred within 30 seconds of contact with the AF sample (Figure 2A,B). After 2 minutes, the membrane continued to grow toward the PAK3 solution with rapid diffusion of molecules from the AF sample through the interface and into the PAK3 membrane (Figure 2C). After 5 minutes, the membrane became denser resulting in a plug (Supporting information) that remained stable in culture for up to 4 days (Figure 2E). Cross-sectional analysis of the plug macrostructure by SEM revealed a multi-layered hierarchical structure (Figure 1F) with highly aligned nanofibres on the surface (Figure 2G) and a randomly arranged bundled network inside the plug (Figure 2H).

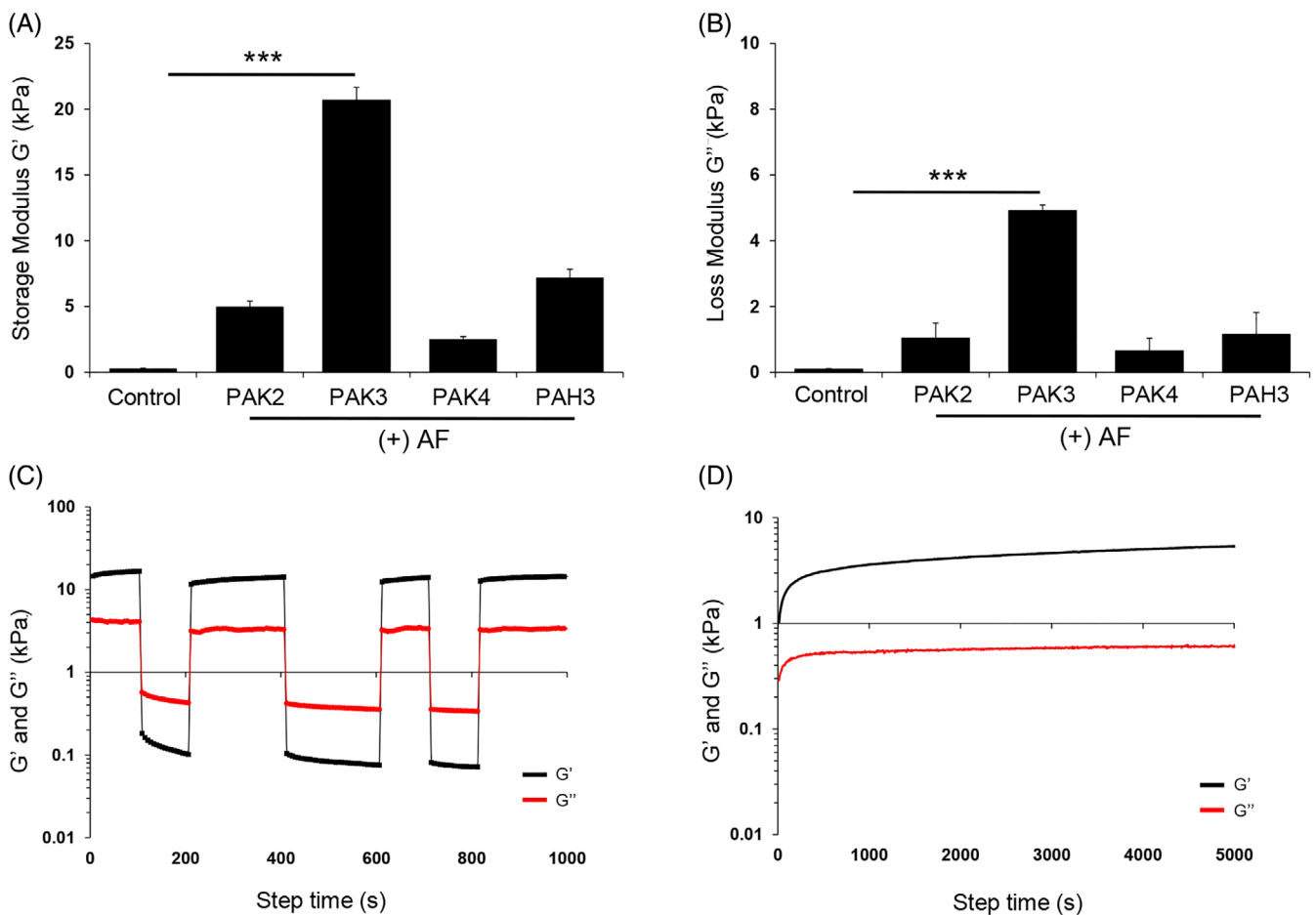


FIGURE 3 Mechanical properties of the PA plugs. The Storage (G') and Loss Modulus (G'') of the plugs were examined after co-assembly of PAK2, PAK3, PAK4, and PAH3 with mid-gestational AF (A and B, respectively). Representative step-strain measurements with applied oscillatory strain alternating between 0.1% and 100% strain for up to 400 seconds at a constant frequency of 1 Hz (C) and time-dependent dynamic oscillatory sweep profiles (D). Error bars in A and B represent the mean and SEM values for $n = 6$ to 15 replicates where $***P < .001$. The AF samples were taken from nine separate donors at $16 + 1$ to $24 + 0$ weeks of gestation and the measurements in C and D, repeated at least three times [Colour figure can be viewed at wileyonlinelibrary.com]

Early and late fixation confirmed an interconnected network of individual and bundled nanofibres arranged in random orientations which increased in density after 30 seconds, 2 minutes and 24 hour (Figure 2I-K).

3.2 | Mechanical properties of the PA plugs

Time-resolved rheological assessment of the PAK3 plugs were compared with PAK2, PAK4, PAH3 and controls formed with a solution of PAK3 and PBS only (Figure 3). The Storage Modulus (G') of the PAK3 plugs had the highest value of 15.8 kPa and was significantly greater when compared to control values of 0.33 kPa ($P < .001$; Figure 3A). In contrast, the PAK4 plugs had the lowest G' value of 2.55 kPa with

PAK2 and PAH3 having G' values of 4.95 and 7.38 kPa, respectively (Figure 3A). A similar profile was found for the Loss Modulus (G'') with values that were significantly greater for the PAK3 (4.92 kPa) plugs when compared to the control (0.08 kPa) specimens ($P < .001$; Figure 3B). Similar to the G' values, the G'' values for PAK2, PAK4 and PAH3 plugs were low and ranged from 0.65 to 1.15 kPa and the values were broadly similar to controls (Figure 3B).

In separate experiments, we investigated the mechanical behavior of the PAK3 plug formation (Figure 3C,D). Step-strain rheographs with applied oscillatory strain alternating between 0.1% and 100% showed rapid self-recovery of the plug up to 1000 seconds (Figure 3C). Time sweep measurements at 0.5% strain showed that the PAK3 plugs attained a G' value of around 8 kPa from 160 seconds that could be maintained up to 5000 seconds (Figure 3D).

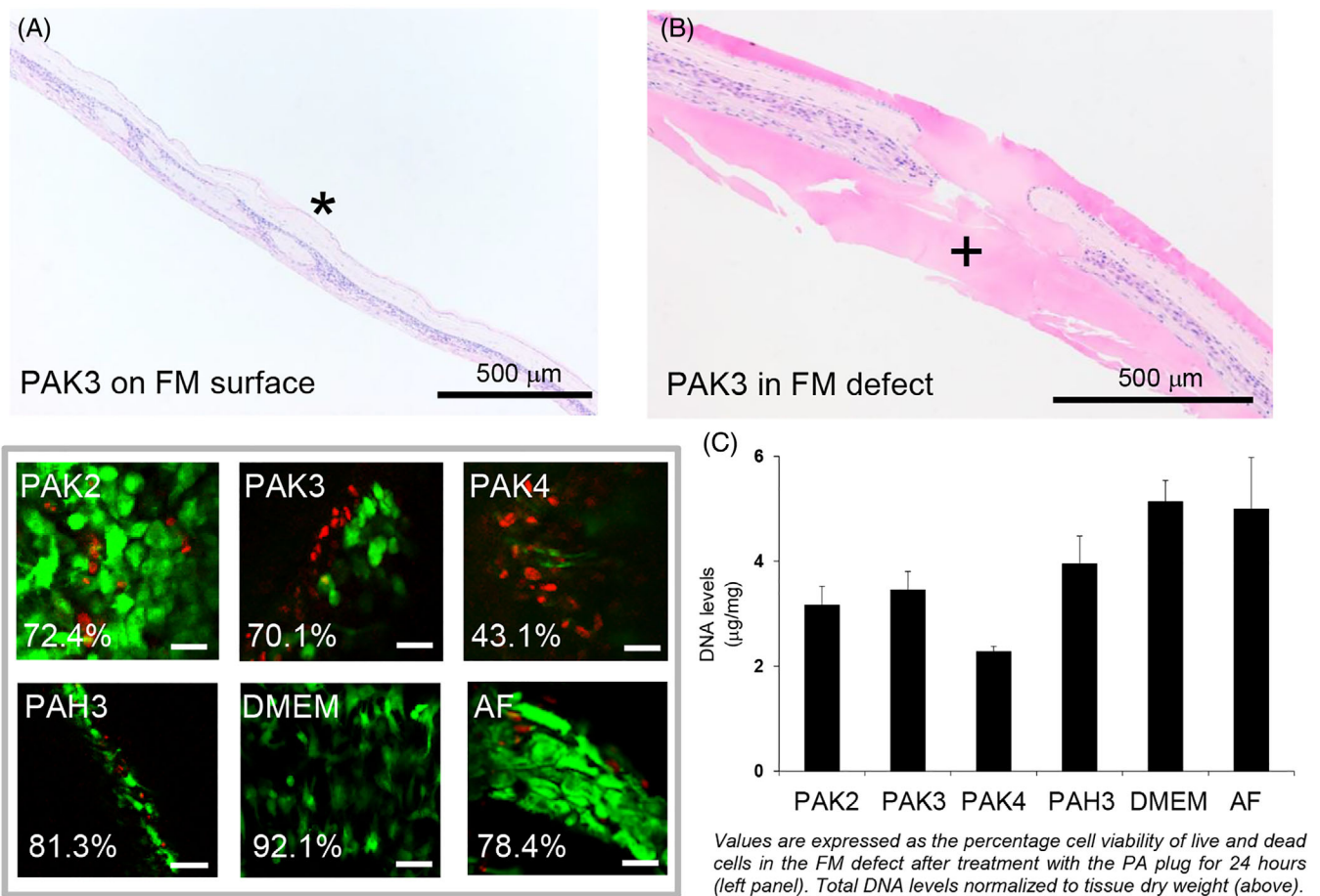


FIGURE 4 Histological examination and cell viability of the PAK3 plug after sealing. A solution of PAK3 was administered directly over the fetal membrane (FM) defect after trauma and cultured for 24 hours. After application, closure was examined in cross-sections of the wounded FM specimens by H&E staining. In the absence of a wound A, the application of PAK3 resulted in a layer of PAK3 (*) on the surface of the tissue. The defect in the FM could be closed with the PAK3 plug without any obvious damage to the integrity of the tissue after PAK3 application (B). Inset shows the percentage cell viability of the FM defect after 24 hours culture with the PA plug with representative confocal images for the effects of PAK2, PAK3, PAK4, and PAH3 compared to controls (DMEM +20% FCS or AF specimen). Total DNA levels were normalized to dry weight after 24 hours of culture in DMEM +20% FCS and are presented in C, where error bars represent the mean and SEM values for $n = 6$ replicates from three donors after elective cesarean section delivery. The cross in B, indicates the PAK3 application site to the FM defect. Scale bar are indicated by white lines, with regions of higher magnification [Colour figure can be viewed at wileyonlinelibrary.com]

3.3 | Effect of PAK3 application to FM defects after trauma

Histological analysis of H&E stained cross-sections of the FM showed a thin coating of PAK3 on the side of the amniotic

membrane (AM) surface (Figure 4A). After application of the FM defect with PAK3, H&E staining revealed a visible plug that formed through the wound and created a layer either side of the AM or chorionic membrane (CM) surface (Figure 4B). After 24 hours, incubation of the FM defect with PAK2, PAK3, or PAH3

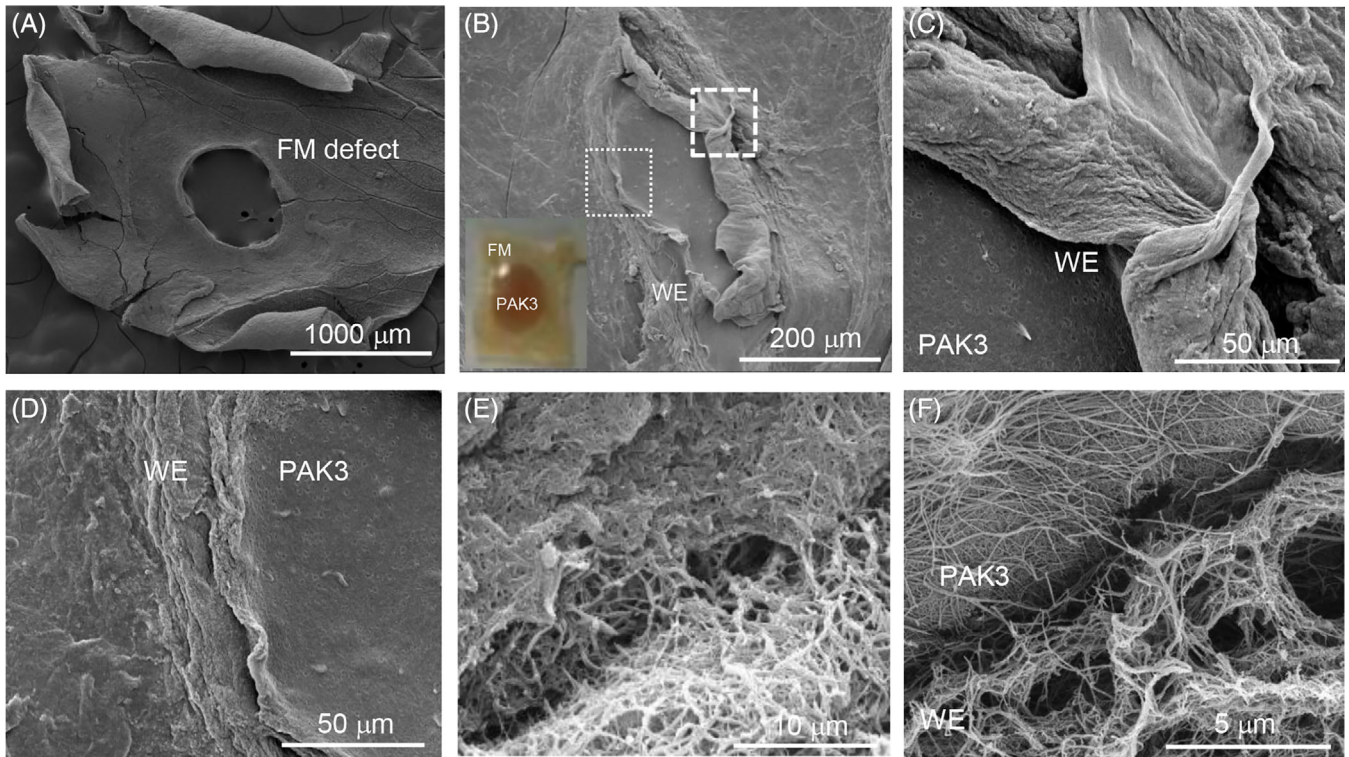


FIGURE 5 Electron micrographs of the FM defect after PAK3 application. The FM explants were traumatized with a needle to create a 0.8 mm hole. There is no evidence of healing after 24 hours of culture with AF (A). Application of PAK3 to the FM defect showed sealing at the edges of the wound (B) and integration of the plug in two regions at higher magnification after 24 hours culture (C and D). Microstructure analysis revealed integration of the edges of FM defect with the PAK3 nanofibrous network (E and F). Scale bar are indicated by white lines, with regions of higher magnification (dotted white lines in B) [Colour figure can be viewed at wileyonlinelibrary.com]

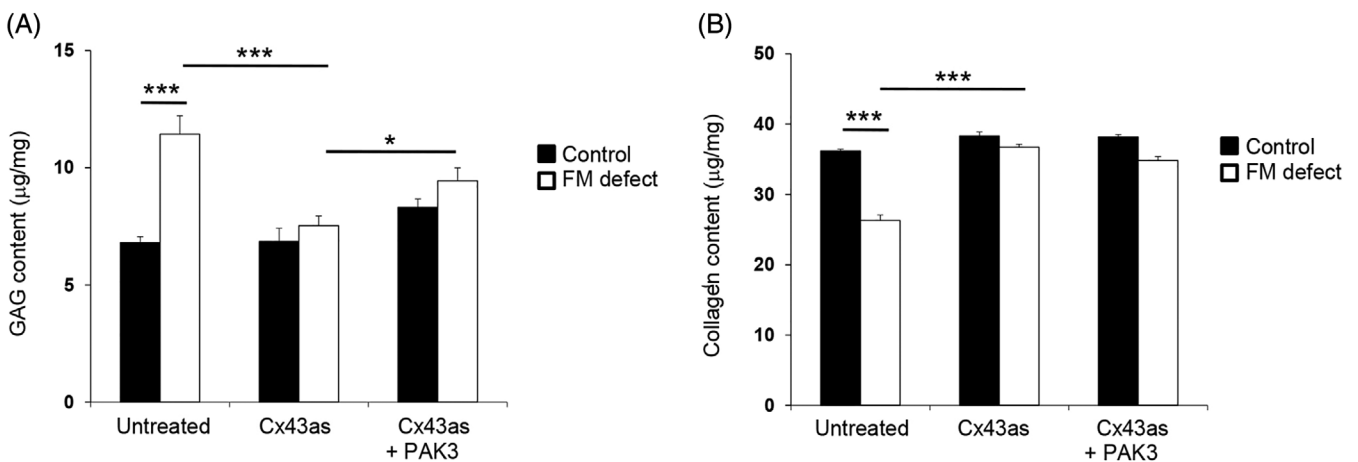


FIGURE 6 The effects of co-culture of FM defects with the Cx43 antisense and/or PAK3 on GAG and collagen content. Control (no hole) and FM defects were cultured in the presence and absence of 50 µM Cx43 antisense and/or PAK3 for 48 hours. At the end of the experiment, the tissues and media samples were analysed for GAG (A) and collagen content (B) by biochemical assay. All values represent the mean and SEM of n = 6 replicates from two separate donors

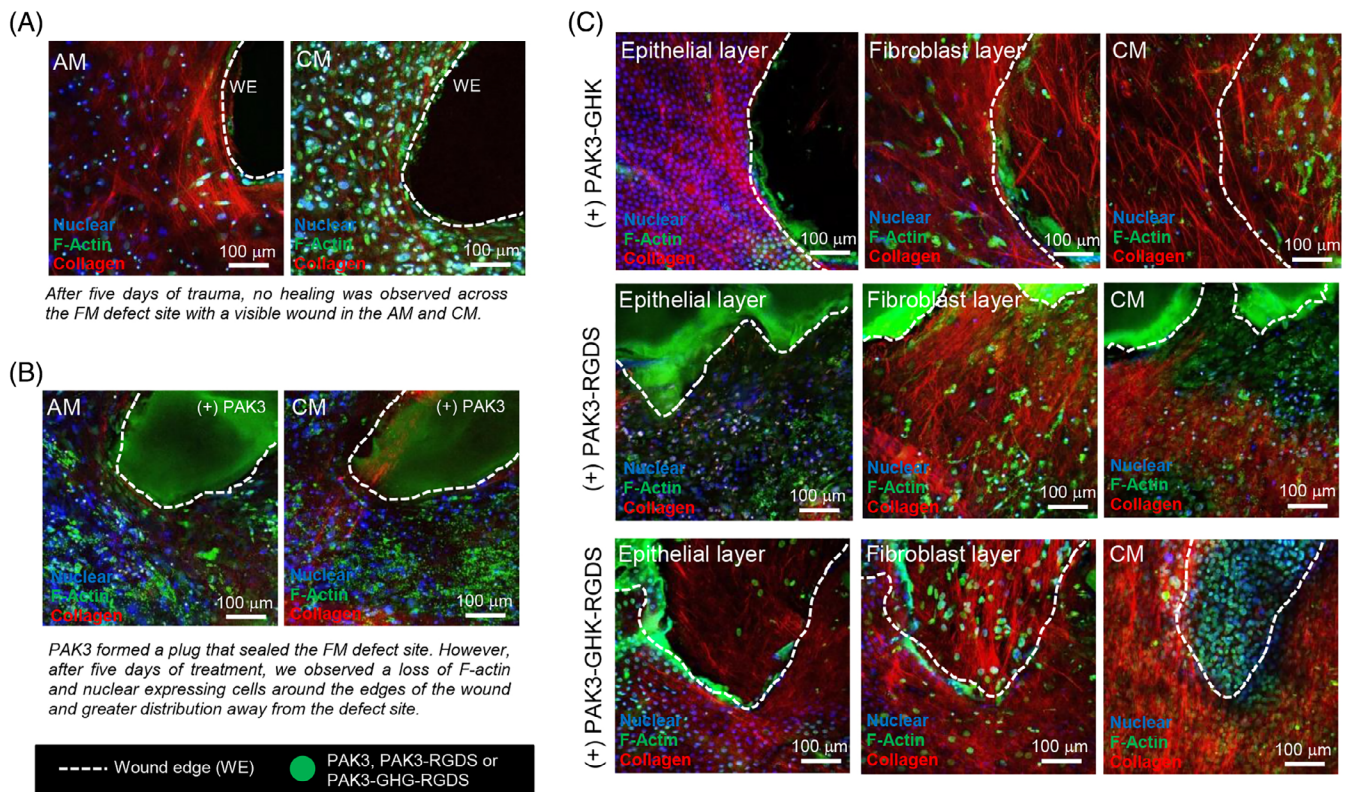


FIGURE 7 IMF confocal microscopy and SHG analysis of the FM defect after in vitro culture with functionalized PAK3. The FM defects were cultured in the absence (A) or presence of PAK3 molecules (B) modified to incorporate the cell-adhesion (RGDS), migratory (GHK) or regenerative (GHK/RGDS) peptides (C) and cultured for up to 5 days after trauma. Cells and nuclei were stained with F-Actin (green) or with DAPI (blue), respectively and SHG imaging of collagen fibers (red). The dotted white lines represent the wound edge (WE) around the FM defect site. All scale bars are indicated by white lines [Colour figure can be viewed at wileyonlinelibrary.com]

maintained cell viability with broadly similar values ranging from 70.1 to 81.3% (inset, Figure 4) compared to AF sample alone or media controls (78.4% and 92.1%, respectively). In contrast, cell viability after PAK4 treatment reduced to 43.1% with fluorescence images showing a greater intensity of non-viable cells. In addition, PAK4 had the lowest DNA value of 2.2 μg/mg compared to PAK2, PAK3, PAK3 which had broadly similar values (3.1–3.9 μg/mg) to the AF alone and media controls (5.1 and 4.99 μg/mg, respectively, Figure 4C).

3.4 | Microstructure analysis after PAK3 application

Application of the FM defect with PAK3 after 24 hour incubation is shown in Figure 5. Analysis by SEM showed a visible defect of around 0.8 mm in diameter with no spontaneous migration of cells into the wound (Figure 5A). Application of the FM defect with PAK3 resulted in the formation of a plug that appeared to seal the edges of the wound (Figure 5B). At higher magnification, we observed integration of the PAK3 plug in two regions of the wound edge (Figure 5C,D). Microstructure analysis revealed a multi-layer nanofibrous network

with elongated and bundled nanofibres that appeared to interconnect with the FM (Figure 5E,F).

3.5 | Combined effects of PAK3 and Cx43 antisense

Figure 6 examined the combined effects of the Cx43 antisense on GAG and collagen levels in control (no defect) and FM defects after PAK3 application for 48 hours. The levels of GAG were significantly higher in FM defect (11.4 μg/mg) than controls (6.8 μg/mg; $P < .001$; Figure 6A). In the presence of the Cx43 antisense, culture alone or in combination with PAK3 significantly reduced the levels of GAG from 11.4 to 7.5 μg/mg ($P < .001$). Co-culture with the antisense and PAK3 marginally reversed this effect with values increasing from 7.5 to 9.4 μg/mg when compared to defects treated with the antisense alone ($P < .05$; Figure 6A). In contrast, the levels of collagen were significantly lower in the FM defect (29.6 μg/mg) than controls (36.2 μg/mg, $P < .001$; Figure 6C). The presence of the Cx43 antisense reversed this effect with the collagen levels increasing from 29.6 to 36.7 μg/mg. However, co-culture with the antisense and the PAK3 had produced no further effects.

3.6 | Morphological and structural changes after application with bioactive PAK3

Figure 7 shows cell morphology and collagen microstructure around the wound edge of the FM defect after 5 days of culture with PAK3 conjugated to RGDS and/or GHK by IMF confocal microscopy and SHG imaging. In control specimens, the FM defect showed a visible wound with no growth of tissue into the defect site after 5 days of trauma (Figure 7A). In wounded AM and CM, we observed a dense region of polarized F-actin expressing cells with nuclear contraction that had migrated toward the edge of the wound. Examination of the collagen structure by SHG imaging showed the presence of highly polarized fibers with a greater intensity of the signal close to the wound edge in the AM compared to the CM. Whilst PAK3 application after 5 days culture formed a plug around the defect site, we observed loss of the collagen signal with a disruption of F-actin and nuclear expressing cells around the edges of the wound and minimal cell adhesion to the plug surface (Figure 7B).

PAK3 functionalised with GHK showed amniotic epithelial cell migration toward the wound edge (Top panel, Figure 7C). In the fibroblast layer and CM, we observed polarized F-actin cell migration toward the edges of the wound and the presence of a discrete network of polarized collagen fibers across the defect site (Top panel, Figure 7C). PAK3 conjugated to RGDS appeared to produce a visible plug that sealed the defect site but there was no cell migration or collagen signal across the biomaterial (Middle panel, Figure 7C). In contrast, FM defects cultured with PAK3-GHK-RGDS showed F-actin amniotic epithelial cell migration and nuclear contraction toward the edges of the wound in the epithelial layer with some evidence of collagen fiber formation across the defect site in the fibroblast layer and in the CM (Bottom panel, Figure 7C). The intensity of the SHG signal closest to the wound edge and in the defect site was increased in the fibroblast layer with the presence of nuclear contraction and F-actin expressing mesenchymal cells (Bottom panel, Figure 7C). In addition, trophoblast like cells had populated the defect site in the CM with the presence of polarized collagen along the edges of the wound.

4 | DISCUSSION

The present study explored the *in vitro* molecular assembly of PAs with human AF to potentially seal and repair defects in the FM after trauma. In this study, we chose one sequence (PAK3) for evaluation in the FM defect model, since this peptide was previously shown to be effective in promoting cell adhesion, migration and proliferation after peptide self-assembly with crosslinked nanofibres that did not affect cytotoxicity and formed plugs with good mechanical properties.^{28,31,32}

We observed strong electrostatic interactions between the positively charged PAK3 and AF molecules to form a solid membrane at the PAK3-AF interface when compared to PAK2, PAK4, and PAH3 which formed soft, liquid or paste-like gels that disintegrated after 6 hours of culture. However, cell viability and mechanical properties were dependent on the physical properties of the peptides, with the PAK2

system resulting in a weak plug despite having the highest values for cell viability (>80%). This is in contrast to PAK3 which mechanically was more stable but had a reduced cell viability of around 70%. Electron micrographs and histological analysis showed potentially morphological sealing at the FM defect site revealing interactions between the self-assembled PAK3 nanofibre and the ECM network. Importantly, we observed F-actin cell and nuclear contraction, mesenchymal cell migration and collagen polarization in the wound edge of the FM after trauma and these responses were enhanced after culture with the PAK3/GHK/RGDS plug alone or in combination with PAK3 and the antisense. In particular, the Cx43 antisense promotes tissue remodeling mechanisms with a reduction in GAG content associated with an increase collagen. The biochemical changes have the potential to for greater cross-linking of the collagen network and could maintain membrane homogeneity and repair in the FM defect. These differences will affect cellular processes, mechanotransduction and repair.^{33,34} We speculate a combination of inflammatory and mechanical factors could perturb typical mechanotransduction processes mediated by Cx43 signaling. Cx43 could therefore be a potential therapeutic target to prevent inflammation and promote tissue remodeling to repair FM defects.

The PAs were designed to have different charge densities and hydrophobicity-hydrophilicity balance in order to maximize interaction with the AF biomolecules, and to obtain plugs with viscoelastic properties capable of sealing defects. The present study showed spontaneous self-assembly of the PAs when in contact with the AF microenvironment, and revealed a dense mesh of fibers to form a plug that sealed the FM defect 24 hours after trauma. Whilst the thickness of the individual and randomly organized nanofibre network appeared to be in the 80 to 100 nm range, it was difficult to confirm whether they mimicked the 3D microenvironment found in the extracellular matrix. Histological and confocal analysis revealed PAK3 formed a layer either side of the FM defect which had poor integration to the edges of the wound suggesting limitations with this particular peptide. In addition, the defect size examined in the present study utilized a 21G needle which created a 0.8 mm defect size that is typical for amniocentesis and intrauterine transfusion. In contrast, the fetoscopic procedures are performed with 3 to 5 mm cannula with often the defect size larger than cannula. The integrity of the PAK3 bonding properties to seal and repair a larger defect size is not known and warrants further investigation. For example, in order to control self-assembly with tunable mechanical properties for larger defects, future work will need to improve both the viscous and elastic properties of the plug in a gradient manner to facilitate adhesion, contraction and efficient migration of cells responding to both the surface of the nanofibres and deformation of the material in a size dependent manner.³³ This could be achieved with ligands such as RGDs to improve actin cytoskeletal dynamics and mechanotransduction of cellular cues and synthesis of structural proteins such as elastin, collagen or fibronectin that will improve mechanical resilience, functionality and matrix viscosity.³⁴⁻³⁶

Under the current experimental conditions, the peptide nanofibrous network is too soft and viscous to facilitate F-actin

nuclear contraction and surface cell mechanics due to the limited surface stiffness of the material to support the typical purse-string contraction mechanism, as previously described.¹⁷ In contrast, recent self-assembling membrane systems were designed to promote protein conformational changes that guide assembly to form soft biomaterials or are triggered by fibronectin to form nano sized networks.^{31,36,37} By controlling the rate of self-assembly in a spatial and temporal manner, this process should engineer a gradient of mechanical properties that influences cell mechanics and drives regeneration. Many soft and hard tissues contain gradients in composition and this is a mechanism that should be explored further.

There have been several previous studies that have described the use of synthetic materials or medical adhesives as promising agents to seal FM defects. However, the link between Cx43 expression and tissue healing has only recently been established and the results of sealing membranes with biomaterials have been variable.^{8,10,11} One difficulty is that there is no ideal in vivo model which allows examination of the synthetic material in a challenging wet and highly charged AF microenvironment. Model systems for in vitro performance assessment should be designed to include attachment of the membranes to the uterine wall since membrane bonding will accomplish greater tensile strength and firm adhesion. Whilst PAs have been previously shown to be effective in promoting healing properties and regeneration of skin wounds in mice, the peptides could have applications in improving adhesion, bonding and cell migration in the FM defect to the uterine wall.³⁸

5 | CONCLUSIONS

The present study investigates novel strategies to seal FM defects using self-assembly peptides such as PAK3. We show that functionalizing the PAK3 with bioactive sequences or culturing with antisense improves sealing and the repair of defects in the FM. However, the mechanical tolerance, cell mechanics and cytotoxicity of the wound after application of the PAK3-AF system needs to be improved before clinical translation can be considered with Cx43 antisense. Future biomaterials will need to be examined in vitro with microfluidic or bioreactor systems that can apply physiological stretch to the defect after treatment.

ACKNOWLEDGEMENTS

The authors thank Dr Aumie Keethes and Nazira Tasnim (QMUL) for analysis. ALD is funded by the National Institute for Health Research at the University College London Hospitals Biomedical Research Centre.

This work was supported by Sparks (17QMU01, TTC), the Rosetrees Trust (M808, TTC), KU Leuven University Fund (JD) and the Prenatal Therapy Fund, University College London Hospital Charity (ALD).

CONFLICT OF INTEREST

The authors declare no potential conflict of interest.

AUTHOR CONTRIBUTIONS

David W. Barrett, Babatunde O. Okesola, Eleni Costa, Anna L. David and Tina T. Chowdhury conceived and designed the study. Jan Deprest, Alvaro Mata, David L. Becker, Anna L. David and Tina T. Chowdhury formulated the research questions. David W. Barrett, Babatunde O. Okesola, Eleni Costa, Chris Thrasivoulou, David L. Becker, Anna L. David and Tina T. Chowdhury, were responsible for data management and statistical analysis. David W. Barrett, Babatunde O. Okesola, Eleni Costa, Chris Thrasivoulou, Alvaro Mata, Anna L. David and Tina T. Chowdhury analysed the data. David W. Barrett and Tina T. Chowdhury drafted the paper, which was revised and approved by all authors. David W. Barrett, Alvaro Mata, Jan Deprest, Anna L. David and Tina T. Chowdhury contributed by revising the manuscript and providing important input. All authors had final approval of the submitted and published versions.

DATA AVAILABILITY STATEMENT

The data that supports the findings of this study are available from the corresponding author upon request.

ORCID

Jan A. Deprest  <https://orcid.org/0000-0002-4920-945X>

Tina T. Chowdhury  <https://orcid.org/0000-0003-4167-7782>

REFERENCES

1. Gratacós E, Sanin-Blair J, Lewi L, et al. A histological study of fetoscopic membrane defects to document membrane healing. *Placenta*. 2006;27:452-466. <https://doi.org/10.1016/j.placenta.2005.03.008>.
2. Sacco A, Ushakov F, Thompson D, et al. Fetal surgery for open spina bifida. *Obstet Gynaecol*. 2019;21:271-282. <https://doi.org/10.1111/tog.12603>.
3. Quintero RA, Morales WJ, Allen M, Bornick PW, Arroyo J, LeParc G. Treatment of iatrogenic previable premature rupture of membranes with intra-amniotic injection of platelets and cryoprecipitate (amniopatch): preliminary experience. *Am J Obstet Gynecol*. 1999;181:744-749. [https://doi.org/10.1016/S0002-9378\(99\)70522-3](https://doi.org/10.1016/S0002-9378(99)70522-3).
4. Liekens D, Lewi L, Jani J, et al. Enrichment of collagen plugs with platelets and amniotic fluid cells increases cell proliferation in sealed iatrogenic membrane defects in the foetal rabbit model. *Prenat Diagn*. 2008;28:503-517. <https://doi.org/10.1002/pd.2010>.
5. Papanna R, Molina S, Moise KY, Moise KJ Jr, Johnson A. Chorionamnion plugging and the risk of preterm premature rupture of membranes after laser surgery in twin-twin transfusion syndrome. *Ultrasound Obstet Gynecol*. 2010;35:337-343. <https://doi.org/10.1002/uog.7476>.
6. Engels AC, Van Calster B, Richter J, et al. Collagen plug sealing of iatrogenic fetal membrane defects after fetoscopic surgery for congenital diaphragmatic hernia. *Ultrasound Obstet Gynecol*. 2014;43:54-59. <https://doi.org/10.1002/uog.12547>.
7. Bilic G, Brubaker C, Messersmith PB, et al. Injectable candidate sealants for fetal membrane repair: bonding and toxicity in vitro. *Am J Obstet Gynecol*. 2010;202:85.e81-85.e89.
8. Engels AC, Joyeux L, Van der Merwe J, et al. Tissuepatch is biocompatible and seals iatrogenic membrane defects in a rabbit model. *Prenat Diagn*. 2018;38:99-105. <https://doi.org/10.1002/pd.5191>.
9. Devlieger R, Ardon H, Verbist L, Gratacós E, Pijnenborg R, Deprest JA. Increased polymorphonuclear infiltration and iatrogenic amniotic band after closure of fetoscopic access sites with a bioactive

- membrane in the rabbit at midgestation. *Am J Obs Gyn.* 2003;188:844-848. <https://doi.org/10.1067/mob.2003.213>.
10. Mallik AS, Fichter MA, Rieder S, et al. Fetoscopic closure of punctured fetal membranes with acellular human amnion plugs in a rabbit model. *Obstet Gynecol.* 2007;110:1121-1129. <https://doi.org/10.1097/01.AOG.0000284624.23598.7c>.
 11. Mann LK, Papanna R, Moise KJ, et al. Fetal membrane patch and biomimetic adhesive coacervates as a sealant for fetoscopic defects. *Acta Biomater.* 2012;8:2160-2165. <https://doi.org/10.1016/j.actbio.2012.02.014>.
 12. Haller CM, Buerzle W, Kivelio A, et al. Mussel-mimetic tissue adhesive for fetal membrane repair: an ex-vivo evaluation. *Acta Biomater.* 2012;8:4365-4570. <https://doi.org/10.1016/j.actbio.2012.07.047>.
 13. Kivelio A, Dekoninck P, Perrini M, et al. Mussel mimetic tissue adhesive for fetal membrane repair: initial in vivo investigation in rabbits. *Eur J Obs Gyn Rep Biol.* 2013;171:240-245. <https://doi.org/10.1016/j.ejogrb.2013.09.003>.
 14. Devaud YR, Züger S, Zimmermann R, Ehrbar M, Ochsenbein-Köblle N. Minimally invasive surgical device for precise application of bioadhesives to prevent iPPROM. *Fetal Diagn Ther.* 2019;45:102-110. <https://doi.org/10.1159/000487393>.
 15. Coutinho P, Qiu C, Frank S, Tamber K, Becker D. Dynamic changes in connexin expression correlate with key events in the wound healing process. *Cell Biol Int.* 2003;27:525-541. [https://doi.org/10.1016/S1065-6995\(03\)00077-5](https://doi.org/10.1016/S1065-6995(03)00077-5).
 16. Sutcliffe JE, Chin KY, Thrasivoulou C, et al. Abnormal connexin expression in human chronic wounds. *British J Dermatol.* 2015;173:1205-1215. <https://doi.org/10.1111/bjd.14064>.
 17. Barrett DW, Kethees A, Thrasivoulou C, et al. Trauma induces overexpression of Cx43 in human fetal membrane defects. *Prenat Diagn.* 2017;37:899-906. <https://doi.org/10.1002/pd.5104>.
 18. Barrett DW, John RK, Thrasivoulou C, et al. Targeting mechanotransduction mechanisms and tissue weakening signals in the human amniotic membrane. *Sci Rep.* 2019;9:6718. <https://doi.org/10.1038/s41598-019-42379-4>.
 19. Karaçal N, Koşucu P, Çobanlı Ü, Kutlu N. Effect of human amniotic fluid on bone healing. *J Surg Res.* 2005;129:283-287. <https://doi.org/10.1016/j.jss.2005.03.026>.
 20. Yang JD, Choi DS, Cho YK, et al. Effect of amniotic fluid stem cells and amniotic fluid cells on the wound healing process in a white rat model. *Arch Plast Surg.* 2013;40:496-504. <https://doi.org/10.5999/aps.2013.40.5.496>.
 21. Skardal A, Mack D, Kapetanovic E, et al. Bioprinted amniotic fluid-derived stem cells accelerate healing of large skin wounds. *Stem Cells Trans Med.* 2012;1:792-802. <https://doi.org/10.5966/sctm.2012-0088>.
 22. Ghalei S, Nourmohammadi J, Solouk A, Mirzadeh H. Enhanced cellular response elicited by addition of amniotic fluid to alginate hydrogel-electrospun silk fibroin fibres for potential wound dressing application. *Colloids Surf B Biointerfaces.* 2018;172:82-89. <https://doi.org/10.1016/j.colsurfb.2018.08.028>.
 23. Zhang S. Fabrication of novel biomaterials through self-assembly. *Nature Biotech.* 2003;21(10):1171-1178. <https://doi.org/10.1038/nbt874>.
 24. Cui H, Webber MJ, Stupp SI. Self-assembly of peptide Amphiphiles: from molecules to nanostructures to biomaterials. *Biopolymers.* 2010;94:1-18. <https://doi.org/10.1002/bip.21328>.
 25. Ghosh A, Buettner CJ, Manos AA, Wallace AJ, Tweedle MF, Goldberger JE. Probing peptide amphiphile self-assembly in blood serum. *Biomacromolecules.* 2014;15:4488-4494. <https://doi.org/10.1021/bm501311g>.
 26. Chowdhury B, David AL, Thrasivoulou C, Becker DL, Bader DL, Chowdhury TT. Tensile strain increased COX-2 expression and PGE2 release leading to weakening of the human amniotic membrane. *Placenta.* 2014;35:1057-1064. <https://doi.org/10.1016/j.placenta.2014.09.006>.
 27. Capito RM, Azevedo HS, Velichko YS, Mata A, Stupp SI. Self-assembly of large and small molecules into hierarchically ordered sacs and membranes. *Science.* 2008;319:1812-1816. <https://doi.org/10.1126/science.1154586>.
 28. Inostroza-Brito KE, Collin E, Siton-Mendelson O, et al. Co-assembly, spatiotemporal control and morphogenesis of a hybrid protein-peptide system. *Nat Chem.* 2015;7:897-904. <https://doi.org/10.1038/nchem.2349>.
 29. Mendoza-Meinhardt A, Botto L, Mata A. A fluidic device for the controlled formation and real-time monitoring of soft membranes self-assembled at liquid interfaces. *Sci Rep.* 2018;8:2900. <https://doi.org/10.1038/s41598-018-20998-7>.
 30. Okesola BO, Lau HK, Derkus B, et al. Covalent co-assembly between resilin-like polypeptide and peptide amphiphile into hydrogels with controlled nanostructure and improved mechanical properties. *Biomater Sci.* 2020;8:846-857. <https://doi.org/10.1039/C9BM01796H>.
 31. Okesola BO, Wu Y, Derkus B, et al. Supramolecular self-assembly to control structural and biological properties of multicomponent hydrogels. *Chem Mater.* 2019;31:7883-7897. <https://doi.org/10.1021/acs.chemmater.9b01882>.
 32. Derkus B, Okesola BO, Barrett DW, et al. Multicomponent hydrogels for the formation of vascularized bone-like constructs in vitro. *Acta Biomater.* 2020;109:82-94. <https://doi.org/10.1016/j.actbio.2020.03.025>.
 33. Estévez M, Martínez E, Yarwood SJ, Dalby MJ, Samitier J. Adhesion and migration of cells responding to microtopography. *J Biomed Mater Res A.* 2015;103(5):1659-1668.
 34. Cantini M, Donnelly H, Dalby MJ, Salmeron-Sanchez M. The plot thickens: the emerging role of matrix viscosity in cell mechanotransduction. *Adv Health Mater.* 2019;9:1901259. <https://doi.org/10.1002/adhm.201901259>.
 35. Huethorst E, Cutiongco M, Campbell FA, et al. Customizable, engineered substrates for rapid screening of cellular cues. *Biofabrication.* 2019;12:025009. <https://doi.org/10.1088/1758-5090/ab5d3f>.
 36. Sprott MR, Gallego-Ferrer G, Dalby MJ, et al. Functionalisation of PLLA with polymer brushes to trigger the assembly of fibronectin into nanonetworks. *Adv Health Mater.* 2019;8:1801469. <https://doi.org/10.1002/adhm.201970010>.
 37. Radvar E, Azevedo HS. Supramolecular peptide or polymer hybrid hydrogels for biomedical applications. *Macromol Biosci.* 2019;19(1):e1800221. <https://doi.org/10.1002/mabi.201800221>.
 38. Seow WY, Salgado G, Lane EB, Hauser CA. Transparent crosslinked ultrashort peptide hydrogel dressing with high shape-fidelity accelerates healing of full-thickness excision wounds. *Sci Rep.* 2016;7(6):32670.

SUPPORTING INFORMATION

Additional supporting information may be found online in the Supporting Information section at the end of this article.

How to cite this article: Barrett DW, Okesola BO, Costa E, et al. Potential sealing and repair of human FM defects after trauma with peptide amphiphiles and Cx43 antisense. *Prenatal Diagnosis.* 2020;1-11. <https://doi.org/10.1002/pd.5826>